River Delta Morphology: Wave Climate and the Role of the Subaqueous Profile

Abstract. *Application of a comprehensive wave climate program to seven major deltas indicates that deltaic configurations and coastal landform combinations depend to a considerable degree on the wave power adjacent to the shore and on the river discharge relative to wave forces. Nearshore wave power is not correlative with deepwater wave power but, owing to frictional attenuation, is a function of the subaqueous slope. The subaqueous slope, in turn, depends partially on the slope and width of the continental shelf but primarily on the rate at which the river can supply sediments to the nearshore zone. River-dominated configurations result only when the river is able to build flat offshore profiles, which reduce nearshore wave power; where the subaqueous slope is steep, waves reach the shore comparatively undiminished and wave-built forms prevail.*

Shoreline geometries and dominant wave regimes strive to attain mutual adjustment along coasts that are molded primarily by the action of ocean waves (*1*). The coastline strives to develop in such a way as to minimize or eliminate longshore gradients in wave forces; in turn, the sediment budget is balanced by redistribution of longshore and onshore wave forces. The resultant subaqueous and subaerial morphology tends to attain quasi-equilibrium with the long-term wave climate. The reciprocation between this morphology and the wave regime is considerable; depositional patterns depend on the spatiotemporal distribution of wave forces; the latter is a function of subaqueous and shoreline topography. Waves are modified by the bottom through refraction, shoaling (*2*), and frictional attenuation (*3, 4*). To date, in most studies of the relationships between wave forces and landforms the effects of bottom friction on waves have not been considered quantitatively; however, in many instances these effects may exert the dominant control on the magnitude and distribution of wave forces in the nearshore zone.

Near the mouths of large rivers the equilibrium between wave regime and depositional topography is upset by the continued introduction of sediments from a source (river channels) external to the littoral transport system. Resultant forms depend not only on the magnitude and distribution of wave forces but also on the ability of the river to supply sediments. Hence river deltas have a spectrum of configurations and landform combinations ranging from those which have been produced solely by the debouchment of the river, without significant interference from wave activity (for example, digitate prograded distributaries), to those which reflect complete dominance by the waves in distributing sediments and straightening the coastline according to their own design (for example, deltas impounded by barrier islands or spits). Whether forms reflect fluvial or wave dominance depends largely on the ability of the river to supply sediments relative to the ability of waves to rework and redistribute them. For the purpose of obtaining a first-order estimate, the sediment-transporting ability of the river is assumed to be proportional to river discharge (*5*), whereas the ability of waves to rework and redeposit sediments is considered proportional to wave power. In a general sense, then, the greater the river discharge the greater is the wave power required to rework the sediments into a wave-dominated configuration.

As part of a continuing research program aimed at explaining the variability of the major river deltas of the world in terms of their process environments (*6*), we have developed a procedure for analyzing the discharge and wave-power climates of delta coasts from published data, maps, and aerial photographs. Sets of deepwater wave characteristics (specific combinations of direction, height, and period) are obtained from published records or by hindcasting from wind data (*7*) where wave data are unavailable. The average relative frequency of each set of wave characteristics occurring during each month is recorded. These values serve as input to a comprehensive computer program developed to compute the effects of refraction, shoaling, and frictional attenuation incrementally along the wave orthogonal by a finite-difference solution to the equations of Bretschneider (*3*) and Bretschneider and Reid (*4*). Wave-power values are calculated from the changing wave characteristics at each 3-m depth interval from deep water to the 3-m contour. From this depth to the shoreline, calculations are made at 0.3-m intervals. We weight these values according to the relative frequencies of the initial wave conditions and calculate weighted mean power values for each month along different sectors of the coast. The ratio of the average discharge per unit channel width to the

Table 1. Characteristic delta morphologies.

Coastline and river mouth configuration	Delta shoreline landforms	Delta plain landforms
	Mississippi	
Highly indented coastline, multiple extended digitate distributaries—"bird foot"	Indented marsh coastline, sand beaches scarce and poorly developed	Marsh, open and closed bays
	Danube	
Slightly indented with protruding river mouths	Marsh coastline with sand beaches adjacent to river mouths	Marsh, lakes, and abandoned beach ridges
	Ebro	
Smooth shoreline with single protruding river channel	Low sand beaches and extensive spits with some eolian dunes	Salt marsh with a few beach ridges
	Niger	
Smooth, arcuate shoreline, multiple river mouths slightly protruding	Sand beaches nearly continuous along shoreline	Marsh, mangrove swamp, and beach ridges
	Nile	
Gently arcuate, smooth shoreline with two slightly protruding distributary mouths	Broad, high sand beaches and barrier formation with eolian dunes, beach ridges at distributary mouths	Floodplain with abandoned channels and a few beach ridges, hypersaline flats and barrier lagoons near present shoreline
	São Francisco	
Straight, sandy shoreline with single slightly constricted river mouth	High, broad sand beaches with large eolian dunes	Stranded beach ridges and dunes
	Senegal	
Straight coastline with extensive barrier deflecting river mouth, no protrusion	High, broad sand beaches with large eolian dunes	Large linear beach ridges and swales, eolian dunes

average nearshore power per unit crest width yields an index of the sediment-transporting ability of the river relative to the reworking ability of the waves. We refer to this as the discharge effectiveness index. Although this ratio is not dimensionless, relative values and ordering between deltas remain independent of units. However, it should be noted that absolute values have no physical meaning.

We have applied our wave climate analyses to seven of the world's major deltas: Mississippi (United States), Danube (Romania), Ebro (Spain), Niger (Nigeria), Nile (Egypt), São Francisco (Brazil), and Senegal (Senegal). These deltas possess unique morphologies reflecting differing relative degrees of riverine and wave control. In the order listed above they range in configuration from types that are almost totally river produced, through those reflecting approximately equal contributions from riverine and wave forces, to types that are completely wave dominated. Distinguishing morphological characteristics of each delta are listed in Table 1; corresponding mean annual values for deepwater and nearshore wave power, mean annual discharges, discharge effectiveness indexes, and attenuation ratios are presented in Table 2. Table 1 indicates a progressive decrease in river-built features—such as digital distributaries, open bays, broad marshes, and crevasses—and an ascendancy of features—such as beach ridges, dunes, spits, and barrier formations—which are responses to high wave energy. These geomorphic tendencies are not explicable in terms of either deepwater wave power or river discharge (Table 2); however, there is a close correlation with the discharge effectiveness index and, to a slightly lesser extent, with the nearshore wave power.

Notably, the Mississippi has higher deepwater wave power than the Danube, Ebro, and Niger, and the value for the São Francisco is more than twice that of the wave-dominated Senegal. The fact that morphology and nearshore wave power in no way parallel deepwater wave power is of primary significance. This reflects the fundamentally important role of frictional attenuation and the consequently varying degrees of power loss owing to different subaqueous slopes. Attenuation increases with decreasing offshore slope. Figure 1 shows the average offshore slope configuration for each of the seven deltas. Slopes are flat and convex seaward of the low-energy deltas; they increase in steepness and concavity toward the high-energy end of the delta spectrum. Similarly, between sectors of individual deltas steep, concave slopes are contingent with zones of high nearshore wave power. This is consistent with the general tendency for wave-built profiles of equilibrium to be concave (*8*).

Table 2. Mean annual discharge and wave-power climate indexes. Wave-power values are given per centimeter of wave crest. The discharge effectiveness index is normalized to maximum discharge.

River	Wave power (erg/sec)		Discharge rate $\times 10^3$ (m^3/sec)	Discharge effectiveness index	Attenuation ratio
	Deepwater	Nearshore			
Mississippi	1.06×10^8	1.34×10^4	17.69	1.00	7913.3
Danube	2.30×10^7	1.40×10^4	6.29	2.14×10^{-1}	2585.0
Ebro	7.28×10^7	5.09×10^4	0.55	4.87×10^{-2}	1299.5
Niger	6.76×10^7	6.59×10^5	10.90	8.03×10^{-4}	102.8
Nile	1.36×10^8	3.21×10^6	1.47	5.86×10^{-4}	42.46
São Francisco	3.71×10^8	9.97×10^6	3.12	2.37×10^{-4}	37.2
Senegal	1.56×10^8	3.77×10^7	0.77	4.75×10^{-5}	4.16

The extent to which power is lost through friction between deep water and the shore is indexed by an attenuation ratio:

$$P_0 r_s^2 / P_s$$

where P_0 and P_s are the deepwater and shore power values, respectively, and r_s is the refraction coefficient nearest the shore. A value of 1 for this quantity indicates complete conservation of power; values greater than 1 are proportional to the degree to which power is lost. If it is assumed that the bottom roughness is constant, frictional attenuation rates increase as water depth decreases; and, for the most commonly occurring wavelengths, the attenuation ratio depends largely on the bottom slope from a depth of 10 m to the shoreline and to some extent on the dominant wave characteristics and the obliquity of wave approach. Table 2 indicates the general increase in attenuation ratio that corresponds to the decrease in offshore slope, as illustrated in Fig. 1. The high attenuation ratio for the Ebro (relative to offshore slope) is attributable to the high obliquity of wave incidence around most of the delta front. The subaqueous profile fronting a delta can therefore be regarded as a control that determines the power of waves that reach the shore. For any particular regional continental shelf slope, the subaqueous slope will depend on the ability of the river to discharge sediments faster than they can be removed by waves.

We conclude from the analyses so far completed that the morphologies of river deltas are, to a considerable degree, functions of river discharge and the strength of wave forces near the delta shoreline. The latter cannot be assumed to be proportional to the wave power in deep water but depends primarily on the subaqueous profile. Hence, before a river can effectively oppose the sea to develop a river-dominated deltaic configuration it must first build a flat, shallow offshore profile to attenuate incoming waves. The actual subaqueous profile which accumulates in front of a particular delta depends partially on the regional slope

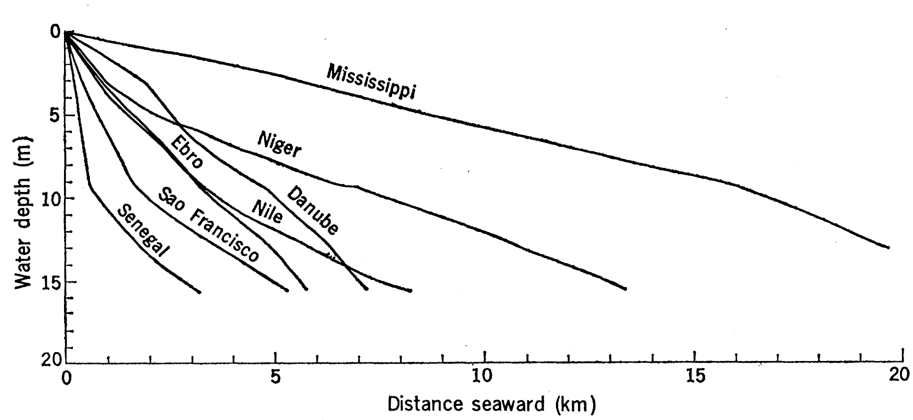

Fig. 1. Average subaqueous profiles of seven deltas.

of the continental shelf but largely on the rate at which the river can supply sediments to the nearshore zone. In summary, wave forces are the primary mechanism whereby the sea reworks and molds deltaic sediments; the construction of flat offshore profiles is the basic mechanism by which the river is able to overcome wave effects.

L. D. WRIGHT
J. M. COLEMAN
Coastal Studies Institute, Louisiana State University, Baton Rouge 70803

References and Notes

1. W. V. Lewis, *Proc. Geol. Ass.* **49**, 107 (1938); J. L. Davies, *Geogr. Stud.* **5**, 51 (1958); J. N. Jennings, *Aust. Geogr.* **5**, 36 (1955); V. P. Zenkovich, *Processes of Coastal Development*, J. A. Steers, Ed. (Wiley, New York, 1967), pp. 383–433; J. Larras, *Plages et Côtes de Sable* (Eyrolles, Paris, 1957).
2. R. L. Wiegel, *Oceanographical Engineering* (Prentice-Hall, Englewood Cliffs, N.J., 1964), pp. 150–179.
3. C. L. Bretschneider, *U.S. Army Corps of Engineers Beach Erosion Board Technical Memorandum 46* (U.S. Army Corps of Engineers, Baltimore, Md., 1954).
4. ——— and R. O. Reid, *U.S. Army Corps of Engineers Beach Erosion Board Technical Memorandum 45* (U.S. Army Corps of Engineers, Baltimore, Md., 1954).
5. Actual sediment transport data are unavailable for most of the rivers examined.
6. J. M. Coleman and L. D. Wright, *Coastal Studies Institute Technical Report 95* (Coastal Studies Institute, Louisiana State University, Baton Rouge, 1971).
7. C. L. Bretschneider, in *Estuary and Coastline Hydrodynamics*, A. T. Ippen, Ed. (McGraw-Hill, New York, 1966), pp. 133–196.
8. V. P. Zenkovich, *Processes of Coastal Development*, J. A. Steers, Ed. (Wiley, New York, 1967), pp. 101–119; J. W. Johnson and P. S. Eagleson, in *Estuary and Coastline Hydrodynamics*, A. T. Ippen, Ed. (McGraw-Hill, New York, 1966), pp. 449–462.
9. Supported by Geography Programs, Office of Naval Research, under contract N00014-69-A-0211-0003, project NR 388 002, with the Coastal Studies Institute, Louisiana State University.

13 December 1971; revised 25 February 1972 ■

Pressure Measurement Made by the Utilization of Ruby Sharp-Line Luminescence

Abstract. *A rapid, convenient technique for precision pressure measurement in the diamond-anvil high-pressure cell, which makes use of the sharp-line* (R*-line) luminescence of ruby, has been developed. The observed shift is* -0.77 ± 0.03 *reciprocal centimeters per kilobar for* R_1 *and* -0.84 ± 0.03 *reciprocal centimeters per kilobar for* R_2 *to lower energy and is approximately linear in the range studied (to 22 kilobars). Line-broadening has been observed in some instances and has been tentatively identified with nonhydrostatic conditions surrounding the ruby sample.*

A persistent deficiency in the routine use of the high-pressure diamond cell (*1*) has been the inability to determine with simplicity and accuracy the pressure on the sample contained between the diamond anvils. In many reports pertaining to the diamond cell, pressures have been determined generally from the applied load on the anvils with no other factors taken into consideration (*2*). This procedure usually results in an unsatisfactory estimate of the pressure, particularly in the higher pressure ranges where errors as large as ± 30 percent have been estimated. Less frequently, pressures in the diamond cell have been determined from lattice parameters of powdered NaCl measured by x-ray diffraction techniques (*3*), and, in at least one instance, pressures were determined from shifts in the optical absorption bands in nickel dimethylglyoxime (*4*). These methods for measuring pressure in the diamond cell are either grossly inaccurate, insensitive, or extremely inconvenient, and it is for these reasons that we think the diamond pressure cell has not realized its full potential as a research tool.

Table 1. Fixed points used to calibrate measurements of pressure in the diamond cell at room temperature.

Substance	Transition*	Transition pressure (kbar)
CCl_4	L-I	1.3
CCl_4	III-IV†	40
H_2O	L-VI	9.6
H_2O	VI-VII	22.3
n-C_7H_{16}	L-I	11.4
C_2H_5Br	L-I	18.3

* The abbreviation L refers to the liquid state, and the Roman numerals designate solid phases. † The III-IV transition point of CCl_4 was not included in the data reported in Fig. 2 because of the nonhydrostatic character of the medium surrounding the ruby sample.

We have discovered what appears to be a new technique for continuous pressure measurement based on the the shift in wavelength of the sharp-line (*R*-line) luminescence in ruby samples. In all of our experiments to date we have used the diamond-anvil apparatus with metal gaskets (*5*), but the method is applicable to any pressure system with optical access. In practice a small fragment of pink ruby crystal (0.05 percent Cr^{3+}, by weight) is placed in the diamond cell with the material under study. The sample is excited by radiation from a super-high-pressure mercury arc which is filtered to eliminate the red wavelengths. A photoelectric detection system is used with a grating monochromator and a strip-chart recorder. A typical luminescence spectrum of a small fragment of ruby contained in the diamond pressure cell at ambient atmospheric pressure and room temperature is shown in Fig. 1, curve A. A similar spectrum is shown in curve B, except that here the pressure on the ruby crystal is approximately 22.3 kbar. The ruby sample from which this spectrum was obtained was enclosed in the diamond cell with an equilibrium mixture of ices VI and VII, a point known to be at 22.3 kbar and room temperature on the equilibrium phase diagram (*6*). The sample chamber, which is defined by the gasket wall and the two diamond anvils, is a right circular cylinder approximately 0.3 mm in diameter and 0.15 mm high. Readily measurable signals can be obtained from ruby samples occupying 20 percent of the cell volume. This amount of ruby does not interfere with other measurements in the cell.

In order to calibrate our measurements in the diamond cell, we have used the freezing points of the liquids listed in Table 1 along with two solid-solid transition points. These materials were selected because they have well-characterized transition pressures and

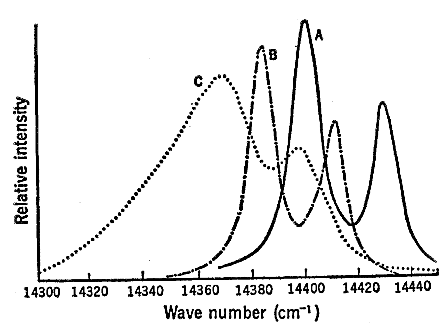

Fig. 1. The *R*-line luminescence spectra of a crystal of ruby in the diamond cell: curve A, ruby sample at ambient atmospheric pressure; curve B, ruby sample in a mixture of ices VI and VII at approximately 22.3 kbar; and curve C, ruby sample in a mixture of CCl_4 III and IV at an average pressure of 40 kbar (nonhydrostatic environment). (Peak heights are arbitrary.)